

# 19.8% efficient “honeycomb” textured multicrystalline and 24.4% monocrystalline silicon solar cells

Jianhua Zhao, Aihua Wang, and Martin A. Green<sup>a)</sup>

*Photovoltaics Special Research Centre, University of New South Wales, Sydney, Australia, 2052*

Francesca Ferrazza

*Eurosolare, Via A. D'Andrea, 6, 00048 Nettuno, Italy*

(Received 27 May 1998; accepted for publication 30 July 1998)

Multicrystalline silicon wafers, widely used in commercial photovoltaic cell production, traditionally give much poorer cell performance than monocrystalline wafers (the previously highest performance laboratory devices have solar energy conversion efficiencies of 18.6% and 24.0%, respectively). A substantially improved efficiency for a multicrystalline silicon solar cell of 19.8% is reported together with an incremental improvement in monocrystalline cell efficiency to 24.4%. The improved multicrystalline cell performance results from enshrouding cell surfaces in thermally grown oxide to reduce their detrimental electronic activity and from isotropic etching to form an hexagonally symmetric “honeycomb” surface texture. This texture reduces reflection loss as well as substantially increasing the cell's effective optical thickness by causing light to be trapped within the cell by total internal reflection. © 1998 American Institute of Physics.

[S0003-6951(98)00840-7]

Multicrystalline (large-grained polycrystalline) silicon wafers prepared by directional solidification have accounted for about 30% of commercial photovoltaic product over recent years. As might be expected from the poorer crystallographic quality, multicrystalline cell performance has lagged considerably behind that of the best monocrystalline devices. The previous best laboratory devices have energy conversion efficiencies of 18.6%<sup>1</sup> and 24.0%,<sup>2</sup> respectively. The crystallographically based, anisotropic surface texturing which is so effective, optically, for monocrystalline cells also generally cannot be applied, contributing to lower performance. Also, the quality of multicrystalline silicon tends to deteriorate during high temperature processing,<sup>3</sup> restricting processing options.

The present letter describes a substantial improvement in multicrystalline silicon cell efficiency to 19.8% by combining honeycomb texturing with multicrystalline material tolerant to high temperature processing. This allows more advanced device structures than previously possible. An incremental improvement in monocrystalline cell performance to 24.4% is also reported.

The 1.5  $\Omega$  cm multicrystalline material used in this work was prepared using a modified directional solidification approach,<sup>4</sup> sawn into wafers and processed into cells of 260  $\mu$ m thickness with the structure shown in Fig. 1. This structure is similar to the PERL (passivated emitter, rear locally diffused) cell developed by the authors' group for monocrystalline substrates.<sup>2</sup> An important feature is the use of thin, thermally grown silicon dioxide layers to almost completely enshroud the cell. This oxide reduces recombination along cell surfaces, improving both the collection probability for carriers photogenerated near the surface and the cell open-circuit voltage (this voltage arises as a balance between pho-

togeneration and recombination). The low refractive index oxide interferes with the action of the double layer ( $\text{MgF}_2/\text{ZnS}$ ) antireflection coating along the cell's top surface (not shown in Fig. 1). Along this surface, the oxide is grown as thin as possible while still retaining the beneficial electronic effects (about 20 nm thickness). Along the rear, the oxide increases internal reflectance and is grown considerably thicker (about 250 nm).

Narrow slots 3  $\mu$ m wide are opened through the top surface oxide to allow metal contact to the cell's  $n$ -type region while small openings (10  $\mu\text{m}^2$ ) on a 250  $\mu$ m grid enable rear  $p$ -type contact. Regions underlying all contacts are heavily doped. This not only reduces contact resistance but also reduces recombination by suppressing minority carrier concentrations near the contact. This suppression is particularly important for the rear contact which would otherwise sink photogenerated carriers and also reduce open-circuit voltage.

The “inverted-pyramid” surface texturing used in monocrystalline PERL cells<sup>2</sup> is not suited to multicrystalline

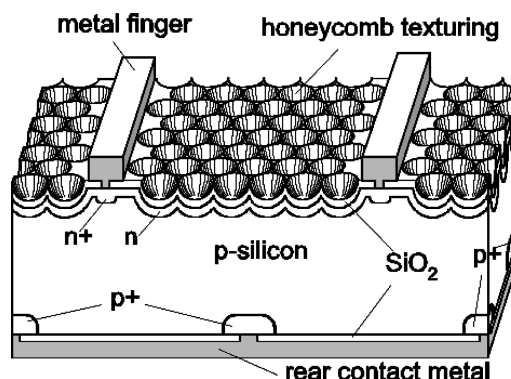
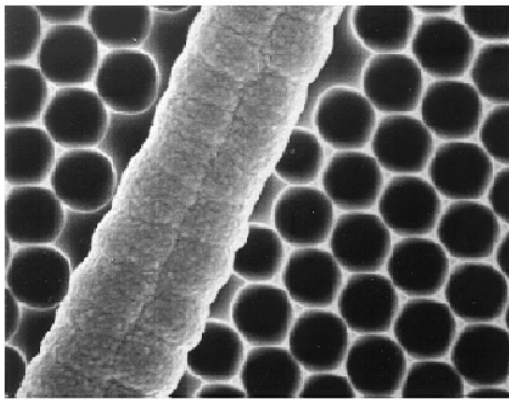
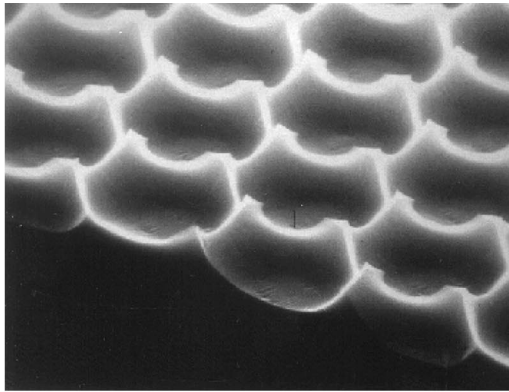


FIG. 1. Schematic of 19.8% efficient multicrystalline silicon solar cell with “honeycomb” surface texturing.

<sup>a)</sup>Electronic mail: m.green@unsw.edu.au



(a)



(b)

FIG. 2. Scanning electron microscopy (SEM) images of close to optimally etched surfaces: (a) plan view, including one of the metallization fingers; (b) perspective view of the texture with enhanced secondary electron emission highlighting the geometry of the thin uppermost regions and cleavage revealing assorted cross sections. The spacing of the hexagons is  $14\ \mu\text{m}$  in both cases.

substrates since it relies on anisotropic etching to expose intersecting  $\{111\}$  crystal planes forming pyramid sides. Such texturing not only reduces front surface reflection but increases the cell's effective optical thickness. Weakly absorbed light is reflected from the cell's rear and strikes the top surface texture internally. Experimentally, the inverted-pyramid structure has been the most effective in trapping this light by total internal reflection, increasing the cell's effective optical thickness by factors as high as 40.

Earlier attempts to implement corresponding structure in multicrystalline cells within our group<sup>5</sup> and elsewhere<sup>6</sup> have been based on etching nominally hemispherical wells into the silicon using the same square matrix layout as for inverted pyramids. The wells are formed by isotropic etching through holes in a masking oxide and approach hemispherical shape if the holes are sufficiently small. Adjacent well regions grow and eventually abut. Limited additional etching beyond this point improves performance slightly by reducing the amount of planar material between wells, at the expense of a reduced height and angle of surface features in overlapping regions.

In this work, hexagonal layouts of oxide holes were used to give superior reflection and light-trapping properties by improving the above trade off. Figures 2(a) and 2(b) show scanning electron microscopy (SEM) images of close to optimally etched surfaces in plan and perspective views, re-

TABLE I. Characteristics of three high performance PERL silicon solar cells. "HEM" and "Eurosil" are multicrystalline silicon wafer material supplied by Crystal Systems and Eurosolare, respectively, while Wacker is float zone monocrystalline silicon wafer material ( $1\ \Omega\ \text{cm}$ ).  $V_{\text{OC}}$ ,  $I_{\text{SC}}$ , FF, and Effic. are open-circuit voltage, short-circuit current, fill factor, and efficiency, respectively. Cell area is  $1\ \text{cm}^2$  for multicrystalline cells and  $4\ \text{cm}^2$  for the monocrystalline device with efficiencies measured on an aperture area and designated illumination area basis, respectively. Measurements by Sandia National Laboratories under standard test conditions (Global AM1.5 spectrum,  $100\ \text{mW}/\text{cm}^2$  intensity,  $25\ ^\circ\text{C}$  cell temperature).

| Cell ID  | Material | Texturing | $V_{\text{OC}}$<br>(mV) | $I_{\text{SC}}$<br>( $\text{mA}/\text{cm}^2$ ) | FF<br>(%) | Effic.<br>(%) |
|----------|----------|-----------|-------------------------|--|-----------|---------------|
| WD3-4B   | HEM      | None      | 643                     | 34.5   | 82.0      | 18.2          |
| WD4-2-4D | Eurosil  | Honeycomb | 654                     | 38.1   | 79.5      | 19.8          |
| WH06-3A  | Wacker   | Pyramids  | 696                     | 42.0   | 83.6      | 24.4          |

spectively. Note the flatter than ideal well bottoms arising from the finite size of holes in the masking oxide ( $\sim 4\ \mu\text{m}$  diam) and the reduced height and angle of features in regions where adjacent wells overlap.

Table I compares the independently confirmed performance of the novel honeycomb cell to that of both an untextured multicrystalline cell of comparable quality<sup>3</sup> and a high performance monocrystalline silicon cell using the standard inverted-pyramid<sup>2</sup> surface texture. The latter establishes a new performance level of 24.4% for a silicon solar cell, incrementally improving the previous value of 24.0% for a similar cell<sup>2</sup> through reduced top metallization losses. The textured multicrystalline device, however, demonstrates a much more significant advantage over previous devices<sup>1</sup> due to texturing and the other high efficiency features of Fig. 1.

Figure 3 compares the wavelength dependent reflection and external quantum efficiency (EQE) of the three cells of Table I. Honeycomb texturing results in reflection generally intermediate between that of the untextured cell and the inverted-pyramid cell, as expected. At the longest wavelengths, silicon becomes transparent and reflection from all three devices increases. Reflection would approach 100% were it not for parasitic absorption within the cell, particularly at the rear reflector. The lower reflection from the textured samples results from increased absorption in this rear reflector due to multiple light passes across the cell. The results suggest light trapping in the honeycomb textured cell

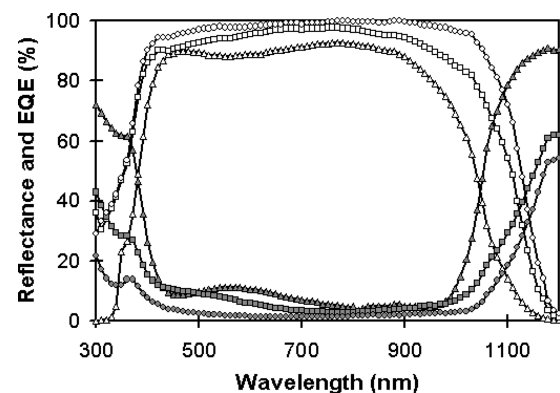


FIG. 3. Hemispherical reflection (lower curves) and external quantum efficiency (upper curves) as a function of wavelength for the three cells of Table I (measurement courtesy of Sandia National Laboratories) ( $\Delta$  planar HEM,  $\square$  honeycomb Eurosil,  $\circ$  textured Wacker).

is comparably effective to that in inverted-pyramid cells.

The differences between EQE at shorter wavelengths are due mainly to differences between top surface reflection from the cells. At longer wavelengths, the planar cell suffers considerably due to poor light trapping. The differences between the textured cells arise primarily from marginally superior optical performance of the inverted-pyramid scheme augmented by the better quality of the monocrystalline material, which ensures that essentially every photogenerated carrier is collected.

More insight into the quality of the textured multicrystalline sample was gained through light beam induced current (LBIC) scanning using weakly absorbed 1060 nm wavelength light (900  $\mu\text{m}$  absorption length). The LBIC scan showed that the response of the 19.8% cell varied between 40% and 100% of peak response in different regions of the cell. The response at this wavelength spatially averaged over the cell area is shown as a single data point in Fig. 3. Since the averaged response is not much lower than that of the high quality monocrystalline cell, it can be inferred that the most strongly responding regions of the multicrystalline cell collect close to 100% of photogenerated carriers.

One surprising result is the exceptional quality of the high response regions even after high temperature processing (above 1000 °C) required to fabricate PERL cells (high temperatures are required to grow the best quality surface oxides and for rear boron contact diffusion). This high temperature tolerance is undoubtedly correlated with modifications to the directional solidification process used to prepare the multicrystalline material.<sup>4</sup> Specifically, equipment changes were made to improve productivity. The shortened cycle time was found to reduce contamination from crucible walls. This may mean that there are fewer mobile impurities in the wafers used in this work to decorate crystal defects or fewer contaminants such as oxygen, known to give rise to subtle high

temperature effects in silicon. Further work will concentrate on identifying the chemical and crystallographic differences between the highest and lowest response regions detected by LBIC scanning. The latter regions do not appear to have been as tolerant of the high temperature treatments as the former. Better control of the properties of these regions will be essential to allow the present results to be reproduced on large area devices. A device on the same wafer as the present, but in an area with a particularly unfortunate arrangement of the latter type of grain, demonstrated efficiency as low as 13.7%.

The authors thank other members of the Photovoltaics Special Research Center for contributions, especially Dr. Mark Gross for SEM photography. They also thank Crystal Systems and Eurosolare for supplying HEM and Eurosil wafers, respectively. Measurements by James Gee and colleagues at Sandia National Laboratories are gratefully acknowledged. The Photovoltaics Special Research Center was established and supported under the Australian Research Council's Research Centres Program. One of the authors (J.Z.) is an Australian Research Fellow supported by the Australian Research Council.

<sup>1</sup>A. Rohatgi, S. Narasimha, S. Kamra, P. Doshi, C. P. Khattak, K. Emery, and H. J. Field, Conference Record of the 25th IEEE Photovoltaic Specialists Conference, New York, 1996 (unpublished), pp. 741–744.

<sup>2</sup>J. Zhao, A. Wang, P. Altermatt, and M. A. Green, Appl. Phys. Lett. **66**, 3636 (1995).

<sup>3</sup>J. Zhao, A. Wang, and M. A. Green, Prog. Photovoltaics **5**, 169 (1997).

<sup>4</sup>F. Ferrazza, A. Endrös, W. Koch, M. Acciarri, S. Pizzini, B. Garrard, I. Dorrity, G. Martinelli, P. Guillo, and F. Caillaud, paper presented at the Second World Conference on Photovoltaic Energy Conversion, Vienna, July 1998 (unpublished).

<sup>5</sup>S. Narayanan, Ph.D. thesis, University of New South Wales, 1989 (unpublished).

<sup>6</sup>M. J. Stock, A. J. Carr, and A. W. Blakers, Sol. Energy Mater. Sol. Cells **40**, 33 (1996).